

A variable coefficient microwave photonic filter based on multi-wavelength fiber laser and Mach-Zehnder interferometer*

CAO Ye (曹晔), LIU Ce (刘策)**, and TONG Zheng-rong (童峥嵘)

Key Laboratory of Film Electronics and Communication Devices, Tianjin University of Technology, Tianjin 300384, China

(Received 19 June 2014; Revised 14 July 2014)

©Tianjin University of Technology and Springer-Verlag Berlin Heidelberg 2014

A microwave photonic filter (MPF) with variable coefficient is proposed and demonstrated, which is constructed by a multi-wavelength fiber laser and Mach-Zehnder interferometer (MZI). Through changing the slope characteristics of Mach-Zehnder interference spectrum adjusted by optical variable delay line (OVDL), the conversion from phase modulation (PM) to intensity modulation (IM) is realized. The multi-wavelength fiber laser with Lyot-Sagnac optical filter has variable wavelength spacing. So the designed filter has a variable number of taps and tap weights. As a result, the tunable range of passband center frequency is 2.6 GHz. The reconfigurability of MPF can be also realized by adjusting the output of fiber laser.

Document code: A **Article ID:** 1673-1905(2014)06-0401-5

DOI 10.1007/s11801-014-4116-5

Most reported microwave photonic filters (MPFs) are needed to work in incoherent condition^[1-3]. The coherent light introduces the nonlinear relationship between the input and output signals. Any tiny change in the radio frequency (RF) system can affect the performance of filter. In recent years, many researches selected various kinds of incoherent sources in MPF experiment. In 2007, Feng^[4] took multi-wavelength fiber laser as optical source, and obtained variable number and position of wavelengths by nonlinear polarization rotation^[5]. In 2011, Zhou^[6] got a multi-tap microwave photonic bandpass filter with center frequency tunable range of 3 GHz by adjusting windowed Fabry-Pérot (FP) filter in multi-wavelength fiber laser. Javier Abreu-Afonso in Universidad de Valencia^[7] achieved a tunable MPF by employing multi-wavelength fiber laser in 2012. But it demanded the erbium fiber to be immersed in liquid nitrogen and the adjustment of FP interferometer, and the complex operation was required. Jiang^[8] sliced wideband optical source by Hi-Bi fiber loop mirror, and obtained an MPF with variable number of passbands in 2013, but the output was highly affected by amplitude noise. Multi-wavelength fiber laser, spectrum slicing and laser array are the best choice for incoherent sources. Among them, the multi-wavelength fiber laser is of low cost and easily tuned. For realizing variable coefficient, the compact optical filter or the two-dimensional (2D) liquid crystal on silicon (LCoS) pixel array^[9] needs high cost,

and the implementation by laser array is complicated.

In this paper, a variable coefficient MPF is proposed and demonstrated based on multi-wavelength fiber laser and Mach-Zehnder interferometer (MZI). The spectrum of MZI has a variable slope to realize positive or negative coefficients. By adjusting optical variable delay line (OVDL) in the interferometer, a bandpass filter with different tap coefficients is obtained. So the MPF has passband with certain tunable range. We further insert a Lyot-Sagnac optical filter in the multi-wavelength fiber laser. Through adjusting polarization controllers (PCs), wavelength spacing is varied. The reconfigurability of MPF can be realized by adjusting output of fiber laser.

Considering the condition under a small signal modulation, if we employ phase modulation (PM) to load the RF signal to a light carrier, the optical field $E(t)$ can be expressed as

$$E(t) = \cos[\omega_c t + m_p V \cos(\omega_m t)], \quad (1)$$

where ω_c denotes the angular frequency of carrier, $m_p V$ denotes the amplitude of modulating signal, and ω_m denotes the angular frequency of RF. Through Eq.(1), the modulation of RF signal is equivalent to a phase change for light carrier. $E(t)$ can be expanded by Bessel functions^[10] as

$$E(t) = J_0 \cos(\omega_c t) + J_1 [\cos(\omega_c + \omega_m)t + \frac{1}{2}\pi] -$$

* This work has been supported by the National High Technology Research and Development Program of China (No.2013AA014200), the National Natural Science Foundation of China (No.61107052), the Natural Science Foundation of Tianjin in China (No.14JCYBJC16500), and the Science and Technology Development Fund Project of Tianjin University (No.2012).

** E-mail: kcl18@126.com

$$J_1[\cos(\omega_c - \omega_m)t - \frac{1}{2}\pi]. \quad (2)$$

The phase modulated signal is composed of two reverse frequencies and phases. If the signal is directly detected by a photodetector (PD), the RF signal cannot be recovered.

The normalized optical transmission spectrum of the unbalanced MZI is shown in Fig.1.

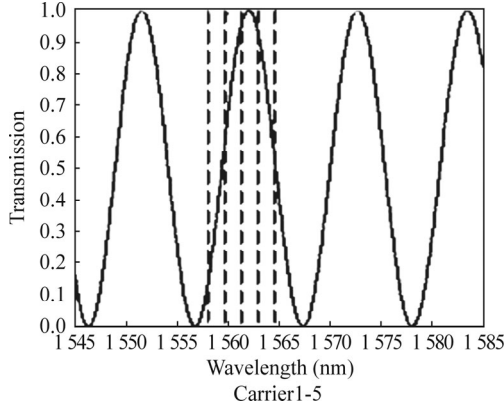


Fig.1 Slope filtering of multi-wavelength fiber laser

We suppose that there are five carriers produced by multi-wavelength fiber laser. The carriers pass through Mach-Zehnder filter and fall into one period of the transmission curve. The same RF signals are modulated on these carriers by PM which introduces instant frequency shift to these carriers. Generated frequency shift is converted to the change of optical intensity. Because the phase modulated signals transfer through the Mach-Zehnder optical filter, the output signals have the similar power and different envelopes. Thus, there are two conditions of tap coefficient polarity, i.e., positive and negative. The polarity of tap coefficient is determined by the wavelength position as

$$\begin{cases} \text{Positive,} & \text{when } \lambda_n - \lambda_1 < \frac{FSR}{2} \\ \text{Negative,} & \text{when } \frac{FSR}{2} < \lambda_n - \lambda_1 < FSR \end{cases}, \quad (3)$$

where $\lambda_1, \lambda_2, \dots, \lambda_n$ denote the output wavelengths of multi-wavelength fiber laser, and FSR stands for free spectrum range of Mach-Zehnder filter.

In our experiment, we choose a long single mode fiber (SMF) as the chromatic dispersion delay line. The recovered RF signal after PD can be expressed as

$$I(t) \propto R[J_0 J_1 \cos(\frac{\omega_c \tau}{2}) \cdot \cos(\frac{(\omega_c + \omega_m)\tau}{2}) \cdot \cos(-\omega_m t - \frac{\pi}{2} + \frac{\omega_m \tau}{2} + \phi_0 - \phi_1) - J_0 J_1 \cos(\frac{\omega_c \tau}{2}) \cdot \cos(\frac{(\omega_c - \omega_m)\tau}{2}) \cdot \cos(\omega_m t + \frac{\pi}{2} - \frac{\omega_m \tau}{2} + \phi_0 - \phi_2)] \propto \sin(\frac{\omega_c \tau}{2}) \cdot \sin(\frac{\phi_1 + \phi_{-1}}{2} - \phi_0) \cdot \cos(\omega_m t + \frac{\phi_1 - \phi_{-1}}{2}), \quad (4)$$

where τ denotes time delay between two optical paths, and ϕ_n denotes the phase delay induced by chromatic dispersion of SMF. Combining Eq.(3) with the property of cosine functions, a relationship between RF spectrum and input RF signal is found as

$$H(f_m) \propto \sin(\frac{\pi \chi \lambda_0^2 f_m^2}{c}) \cdot \sum_{n=1}^N \sin(\frac{\omega_n \tau}{2}) \cdot P_n \cdot e^{-j2\pi f_m (n-1)T}, \quad (5)$$

where χ is the accumulated dispersion of the dispersive device SMF, λ_0 is the central frequency of carrier, f_m denotes the frequency of modulation signal, c is propagation velocity of optical wave, P_n denotes the normalized power of output multi-wavelength lasing, n denotes the number of wavelengths, and T denotes the time difference delay between adjacent wavelengths raised by dispersive device^[11].

Fig.2 shows the experimental structure based on multi-wavelength fiber laser and MZI for variable coefficients. In the configuration of designed MPF, multi-wavelength lasing is produced via a ring cavity. The cavity is composed of an erbium-doped fiber amplifier (EDFA) and a Lyot-Sagnac interferometer. The EDFA has the saturation output power of 1 W. Since the gain-bandwidth of EDFA is limited, the multi-wavelength output has finite taps to form a finite impulse response (FIR) filter. The used polarization maintaining fiber (PMF) has a beat length of 3.1 mm at 1 550 nm. The PCs in the Sagnac interferometer are used to adjust the output wavelength spacing. A 15 km-long SMF is used to weaken the mode competition, so the cavity has a stable multi-wavelength output. The isolator (ISO) enables the light wave to convey along a fixed direction. PC3 adjusts the polarization state of lasing for the reconfiguration of laser output. Laser comes out from the coupler (OC) and passes through another coupler to observe its spectrum by optical spectrum analyzer (OSA). 99% of output taps are modulated by RF signal from a signal generator. The signal processing unit is composed of MZI and SMF. The processed signal is sent to a PD for optical to electrical conversion, and the RF response spectrum is observed by a spectrum analyzer.

We introduce a Lyot-Sagnac optical filter into the multi-wavelength laser for adjusting the wavelength spacing. The Lyot-Sagnac structure is shown in Fig.3. L_1 and L_2 are the lengths of PMF1 and PMF2, respectively. By changing the polarization angle of PC1, we obtain four different output efficient lengths of PMF theoretically, which are $L_1, L_2, |L_1-L_2|$ and L_1+L_2 . The corre-

sponding wavelength spacing varies with the adjustment of PCs. The relationship between wavelength spacing and PMF efficient length is^[12]

$$\Delta\lambda = \frac{\lambda^2}{\Delta n \cdot L}, \tag{6}$$

where $\Delta\lambda$ denotes wavelength spacing, λ is the center wavelength of output lasing, and Δn is the birefringence of PMF. When the fast axis of PMF1 matches the fast axis of PMF2, the maximum efficient length is obtained, and when the slow axis of PMF1 matches the slow axis of PMF2, the minimum efficient length is generated with adjusting PC1. In our experiment, we have two sections of PMF with the lengths of 5.72 m and 11.22 m, respectively. They have the same birefringence and belong to a consistent type.

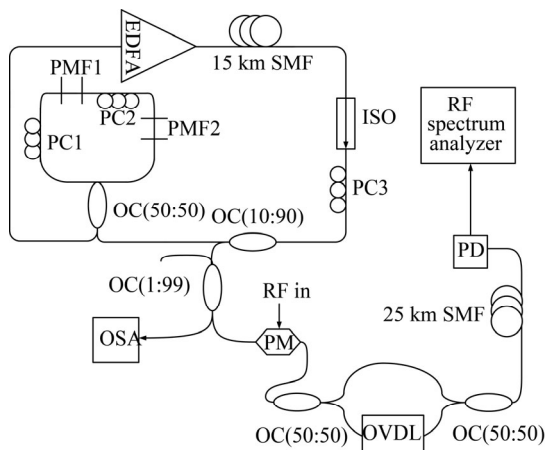


Fig.2 Schematic diagram of the proposed MPF structure

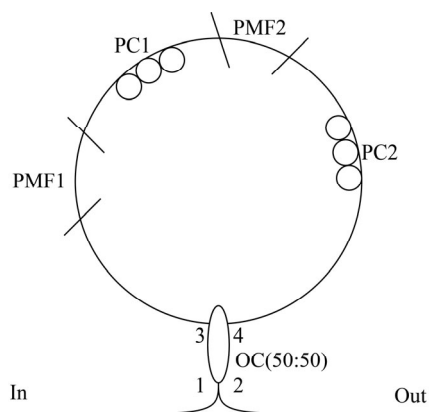


Fig.3 Schematic diagram of the Lyot-Sagnac optical filter structure

The measured amplified spontaneous emission spectrum of EDFA has a wide wavelength range of 37.6 nm. When the fiber laser operates, the wavelength spacing of 0.88 nm is got. By using 25 km-long SMF, our aim is to realize the conversion from PM to intensity modulation (IM) and introducing time delay for the taps. Through the relationship between filter period and wavelength spac-

ing, which is $T=D \cdot L \cdot \Delta\lambda$, where D is chromatic dispersion coefficient, and L is physical length of SMF, a period of 2.6 GHz appears in the spectrum response. By adjusting PC3, a multi-wavelength lasing output is obtained as shown in Fig.4.

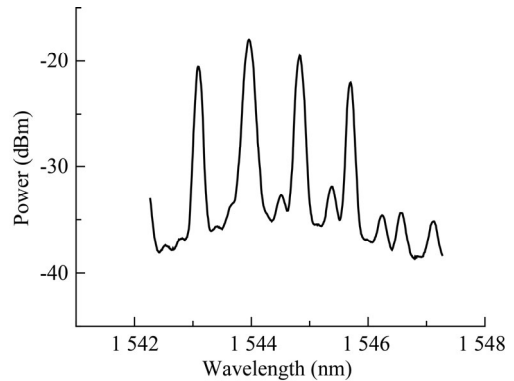


Fig.4 The multi-wavelength laser output with wavelength spacing of 0.88 nm observed by OSA

Uniformly-spaced multi-wavelength lasing appears in the measured spectrum, and the center wavelength of lasing is at about 1545 nm. From theory analysis, we know that the wavelength spacing is in direct proportion to the FSR of filter. Then we normalize the coefficients of taps to get corresponding tap weights. Considering the case without the MZI, when the output multi-wavelength lasing spacing is 0.88 nm, a bandpass filter with FSR range of 2.6 GHz is obtained as shown in Fig.5. We infer from Fig.5 that the PM-IM conversion must be generated, because a notch is observed in baseband location. This approach leads to a bandpass filter without baseband resonance. When we inset the MZI into the experiment system, due to the interferometer is controlled by OVDL, different passband positions appear. The RF response has mainlobe-to-sidelobe suppression ratio (MSSR) of 14.73 dB and 3 dB bandwidth of 1.032 GHz. Comparing Fig.5(a) with (b), only passband position moves, but quality factor and MSSR keep the same.

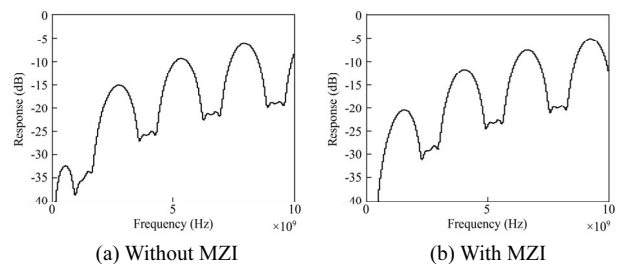


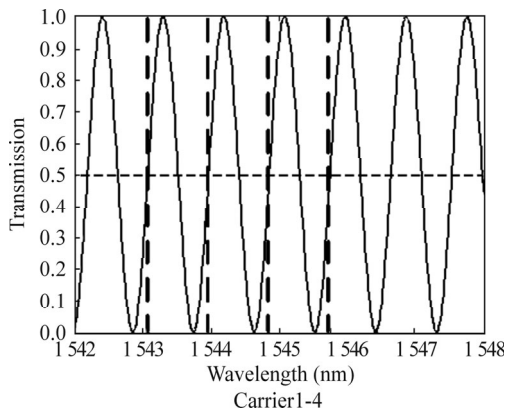
Fig.5 RF responses with 0.88 nm wavelength spacing

The schematic diagrams of RF signal slope filtering with different MZI time delays are shown in Fig.6. Fig.6(a) shows the RF response, in which the MZI has time delay of 6.2 ps and the multi-wavelength lasing falls on the center slope of Mach-Zehnder spectrum, no matter

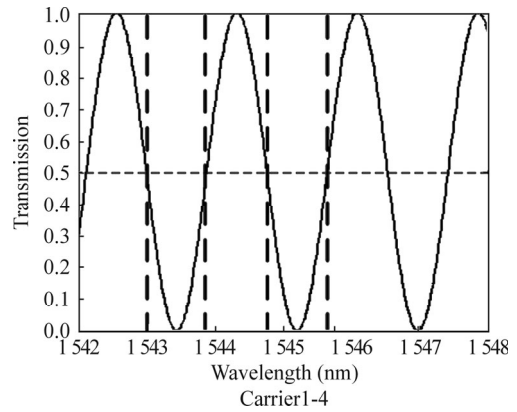
the slope is positive or not, and in formula, the term of $\sin(\omega_c\tau/2)$ equals 1. Right now the coefficient is multiplied by tap weight and term of $\sin(\omega_c\tau/2)$. And when the bias voltage on MZI changes, the output lasing falls on the peak and valley points of Mach-Zehnder spectrum, the term of $\sin(\omega_c\tau/2)$ equals 0, and nothing will be observed in spectrum analyzer. Through analysis in theory, the phase modulated carrier generates the first-order sidebands, and when the carrier falls on the peak or valley of Mach-Zehnder spectrum, its higher sideband and lower sideband suffer the same amplitude influence. There is no RF response in this situation because PM-IM conversion disappears. The fundamental frequency has no resonance, because the 25 km-long SMF has a response of $\sin(\frac{\pi\chi\lambda_0^2 f_m^2}{c})$ and it is 0 at initial frequency.

Therefore, the 25 km-long SMF not only offers the time delay, but also restrains the fundamental frequency response. Fig.5(b) is formed by introducing 3.1 ps time delay difference interferometer, and its passband has the same shape with that in Fig.5(a). The multi-wavelength lasing on interferometer spectrum, whose position is positive or negative slope, is shown in Fig.6. When $\sin(\omega_c\tau/2)$ equals 1 and -1, coefficients as $[-1 \ 1 \ -1 \ 1]$ are generated, and tap coefficient is composed of weight and corresponding coefficients. From the simulated result, we can see that tuning of filter is based on the change of coefficient polar, which is equivalent to that every other tap has a phase variation of π . Hence we get a tunable bandpass filter because of the effect of OVDL. When the bias voltage on the interferometer varies, the moved light spectrum changes the slope filtering feature. When the tap coefficients become 0, nothing can be observed. If the interferometer spectrum has a π phase overturning, coefficients as $[1 \ -1 \ 1 \ -1]$ are generated, and the RF response is the same shape as shown in Fig.5(b). This result explains that the order of tap phase changing doesn't influence the passband shape.

Fig.7 shows the bandpass filter formed by 2 taps when the interferometer has time delay of 1.5 ps, and there are more passbands in 10 GHz frequency range. It is mainly because the efficient taps are reduced and half of taps have coefficient of 0. FSR becomes 1.3 GHz, which decreases by two times of the original one.



(a) 6.2 ps time delay



(b) 3.1 ps time delay

Fig.6 RF signal slope filtering with carriers at different positions

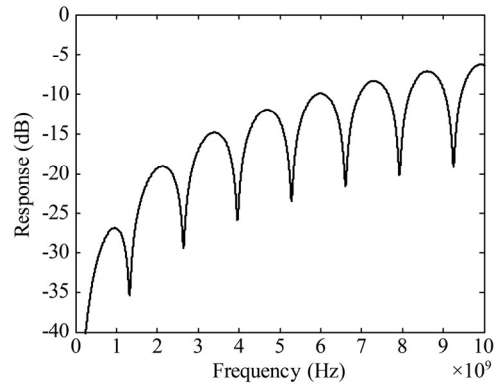


Fig.7 Bandpass filter formed by 2 taps

When there is no bias voltage applied on MZI, 0.44 nm wavelength spacing is obtained by changing the rotating angles of PC1 and PC2. The lasing spectrum has an approximate flat shape, but the middle lasing has the highest power as shown in Fig.8. The 0.44 nm spaced light carrier passes through signal processing unit, and the analysis results are shown in Fig.9. Along with the decrease of wavelength spacing, the number of taps is increased, and the efficient taps become 9. The FSR of filter becomes 5.2 GHz. By tuning OVDL in MZI, the passband position moves. In Fig.9(a), MSSR is 13.365 dB, 3 dB bandwidth is 0.84 GHz, and only one passband exists in 10 GHz frequency range. The filter has MSSR of 12.2 dB which is lower than before due to the multi-wavelength lasing output spectrum is not a regular one. This condition leads to irregular P_n . Right now the MZI has time delay of 12.4 ps. Just at the moment when it turns to 6.2 ps, Fig.9(b) appears. Its passband shape keeps unchanged but the passband position moves by 2.6 GHz. Fig.9(c) and (d) show the spectra with 3.1 ps time delay added in the interferometer, and the number of taps varies with the position of carrier falling on. In Fig.9(c) and (d), MSSRs are 11.55 dB and 7.583 dB, and 3 dB bandwidths are 851 MHz and 829 MHz, respectively. The filter has a reconfigurable feature. We observe from the simulation result that MSSR drops a little and FSR

doubles compared with Fig.9(b). Such a multiband filter can be used in multiplexing technique.

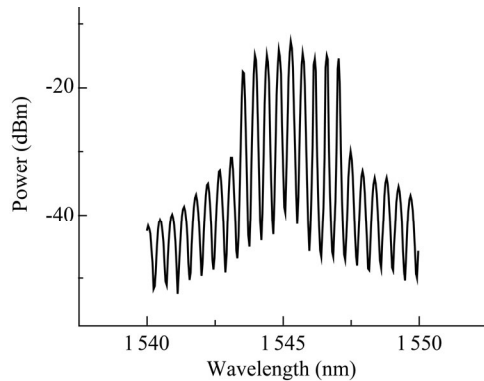


Fig.8 0.44 nm multi-wavelength lasing observed by OSA

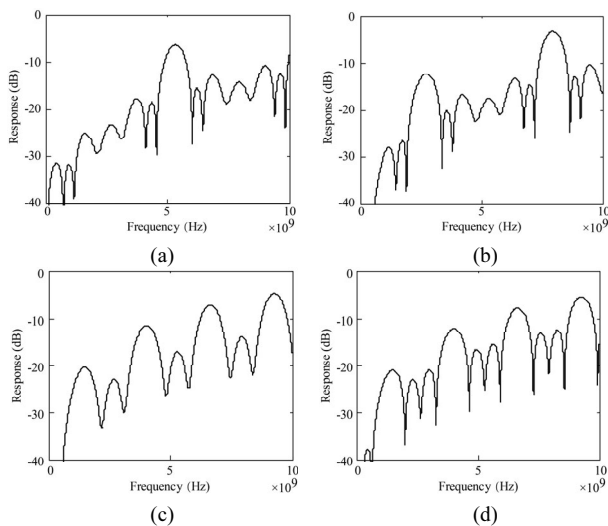


Fig.9 RF responses of 0.44 nm multi-wavelength lasing observed by OSA: (a) 12.4 ps time delay; (b) 6.2 ps time delay; (c) (d) 3.1 ps time delay

We propose a novel variable coefficient MPF composed of multi-wavelength fiber laser and MZI. The fiber laser has a variable multi-wavelength spacing realized by adjusting PCs in resonant cavity, and two types of lasing outputs are obtained. And the MZI in configuration has a

spectrum which can be tuned by OVDL, so the tap coefficient is variable. The filter remains an unchanged shape with the shift of passband center frequency, and its reconfigurability is realized by changing the wavelength spacing and the number of wavelengths.

References

- [1] WEI Zhi-hu, WANG Rong, FANG Tao, PU Tao, SUN Guo-dan and ZHENG Ji-lin, *Journal of Optoelectronics·Laser* **24**, 1086 (2013). (in Chinese)
- [2] ZHANG Cheng, YAN Lian-shan, PAN Wei, LUO Bin, ZOU Xi-hua, JIANG Heng-yun, LU Bing and ZHOU Tao, *Journal of Optoelectronics·Laser* **24**, 1662 (2013). (in Chinese)
- [3] Liwei Li, Thomas X. H. Huang and Robert Minasian, *IEEE Photonics Technology Letters* **26**, 82 (2014).
- [4] Xinhuan Feng, C. Lu, H. Y. Tam and P. K. A. Wai, *IEEE Photonics Technology Letters* **19**, 1334 (2007).
- [5] Xinhuan Feng, Hwa-yaw Tam and P. K. A. Wai, *Optics Express* **14**, 8205 (2006).
- [6] Junqiang Zhou, Songnian Fu, Feng Luan, Jia Haur Wong, Sheel Aditya, Perry Ping Shum and Kenneth Eng Kian Lee, *Journal of Lightwave Technology* **29**, 3381 (2011).
- [7] Javier Abreu-Afonso, Antonio Díez, Jose Luis Cruz and Miguel V. Andrés, *IEEE Photonics Technology Letters* **24**, 2129 (2012).
- [8] Yang Jiang, Perry Ping Shum, Peng Zu, Junqiang Zhou, Guangfu Bai, Jing Xu, Zhuya Zhou, Hengwen Li and Shunyan Wang, *IEEE Photonics Journal* **5**, 5500509 (2013).
- [9] Thomas X. H. Huang, Xiaoke Yi and Robert A. Minasian, *Optics Express* **19**, 6231 (2011).
- [10] Jun Wang, Fei Zeng and Jianping Yao, *IEEE Photonics Technology Letter* **17**, 2176 (2005).
- [11] Fei Zeng and Jianping Yao, *Journal of Lightwave Technology* **23**, 1721 (2005).
- [12] Young-Geun Han, Gilhwan Kim, Ju Han Lee, Sang Hyuck Kim and Sang Bae Lee, *IEEE Photonics Technology Letters* **17**, 989 (2005).